Role of twinning on the omega-phase transformation and stability in zirconium

M. Arul Kumar, Nadege Hilairet, R.J. Mccabe, T. Yu, Y. Wang, I.J. Beyerlein, C.N. Tomé

Role of twinning on the omega-phase transformation and stability in zirconium

M. Arul Kumar,[1]* N. Hilairet,[2] R. J. McCabe,[1] T. Yu,[3] Y. Wang,[3] I. J. Beyerlein,[4] C. N. Tomé[1]

[1]Materials Science and Technology Division, Los Alamos National Laboratory, Los Alamos, NM 87545, USA

[2]Univ. Lille, CNRS, INRA, ENSCL, UMR 8207 – UMET - Unité Matériaux et Transformations, F-59000 Lille, France

[3]Center for Advanced Radiation Sources, The University of Chicago, Chicago, IL, 60637, USA

[4]Mechanical Engineering Department, Materials Department, University of California Santa Barbara, Santa Barbara, CA, 93106, USA

* marulkr@lanl.gov

Abstract

Group-IV transition metal zirconium is used in nuclear and chemical industries as a choice material for operating in extrem\e environments. At ambient-conditions, zirconium has a stable hexagonal-close-packed structure (α-phase), but under high-pressures it transforms into a simple-hexagonal structure (ω-phase). Experimental studies involving high-pressures have reported retention of ω-phase upon recovery to ambient-pressures, which is undesirable since the ω-phase is brittle compared to the α-phase. Understanding the α-to-ω transformation is relevant for enhancing the applicability of transition metals. In this work using in-situ synchrotron X-ray diffraction, we show that deformation twins in the α-phase lower the transformation pressure and increase the amount of retained ω-phase. Our analysis concludes that the characteristics of the stress fields associated with the twins promote the α-to-ω transformation while making the reverse transformation energetically unfavorable. This work reveals a plausible way to design Zr microstructure for high-pressure applications via controlling twinning and retained ω-phase.

Keywords: Phase transformation, High pressure, Zirconium, X-ray diffraction

1. Introduction

Group IV transition hexagonal close packed (HCP) metals (α-phase), such as Ti, Zr, and Hf, undergo structural transformations upon changes in temperature and/or pressure due to the easy transfer of electrons between the *s* and *d* bands [1, 2]. Among them, Zr is particularly attractive for use in aggressive environment applications as it is biocompatible and displays excellent resistance to corrosion and radiation damage. Common present-day applications include biomedical implants and structural components in chemical and nuclear reactors [3]. Increasing temperature transforms the HCP α-phase structure to a body centered cubic (BCC) (β-phase) structure, while increasing pressure transforms it to a simple hexagonal (Hex) (ω-phase) structure [1]. The high-pressure ω-Zr phase is significantly stiffer, more brittle, and more plastically anisotropic than the α-phase [4-7]. Consequently, the properties of post-transformed Zr with retained ω-phase differ significantly compared to those of the α-Zr [7]; among them, yield stress (which goes from 250 MPa to 650 MPa when the ω-phase content increases from 0% to 80%), ultimate strength, and strain hardening.

The martensitic α-to-ω phase transformation has been studied over the last several decades. In these studies, the ω phase was introduced via hydrostatic pressure testing [1, 8-10], shock loading [7, 11], and high-pressure torsion (HPT) [12, 13]. Based on static pressure experiments, the α-to-ω phase transformation has been classified as a hysteresis transformation because, upon removal of the imposed pressure, most of the ω-phase reverses back to the α-phase [5]. Yet interestingly, when the transformation occurs as a result of shock or HPT, a significant fraction of the ω-phase is retained as a meta-stable phase in the α -phase Zr after the high pressure is removed [7, 11, 12]. For example, Cerreta et al. [7] observed around 80% retained ω-phase in shock-loaded Zr, and Perez-Prado et al. [12] observed nearly 100% retained nano-crystalline ω-phase in a HPT Zr-sample. The major difference between shock and HPT conditions versus the static pressure test is that the former methods impose severe plastic deformation, whereas static pressure experiments impose predominantly hydrostatic pressure with negligible deviatoric stress and plastic deformation. It is evident that when plastic

deformation accompanies high pressure, the phase composition and stability of the ω phase is altered. The heterogeneous deformation states associated with shock loading and HPT deformation, combined with limitations imposed by the experimental conditions, make it difficult to study the role of plasticity on phase transformations using either in-situ or ex-situ analysis.

Despite a number of high-pressure experimental studies performed over seven decades, the role of plastic deformation and microstructure on the α-to-ω phase transformation is not well understood [1, 2, 5, 9, 14-16]. Most studies have considered other aspects of the transformation, like effects of pressure medium, pressure rate, impurities, etc. [5, 8, 10, 15, 17]. Three distinctive characteristics of shock loading and HPT conditions are worth noting: (i) both impose significant shear to the material and as such, naturally activate large amounts of twinning in addition to dislocation glide [18, 19]; (ii) postmortem microscopy analysis of shock-loaded Zr shows that the retained α-grains are lath-shaped, which resembles closely the conventional morphology of deformation twins [7, 20]; (iii) atomistic calculations show that under shock loading, coherent twin boundaries in Ti act as favorable nucleation sites for the α-to-ω phase transformation compared to incoherent twin boundaries and random grain boundaries [21]. Taken together, we speculate that under shock loading and HPT conditions, α-grains first twin and then the ω-phase nucleates at or in the vicinity of twin boundaries. Thus, in this work we hypothesize that deformation twins in α-Zr favor the pressure-induced α-to-ω transformation and the stability of the ω phase at ambient condition.

Twins introduce coherent and semi-coherent boundaries into the microstructure. In this light, many boundary-driven phase transformations have been reported such as in polycrystalline Fe (from α-to-ε) [22], rolled Ti (from HCP to FCC) [23], uranium dioxide [24], and the Cu/Ag system [25]. A few studies have linked deformation twinning in β-phase Ti alloys and Zr alloys to the ω-phase transformation[26-28]. Under uniaxial and/or cyclic loading, these β-phase alloys may undergo either β-twinning or the β-to-ω phase transformation, or both, depending on alloying composition. Addition of vanadium in β Ti-16-22%V alloys promotes β-twinning over the stress-induced ω-phase transformation [26]. In Niobium-rich Ti alloys, however, β-twinning and ω-phase

transformation have been observed together [27, 28]. Yet, the role of twinning on the α-to-ω phase transformation is not understood clearly.

In this work through *in-situ* high-pressure X-ray synchrotron experiments, we systematically investigate the effect of pre-existing deformation twins on the α-to-ω phase transformation in pure Zr. Samples are pre-deformed to introduce different amounts of deformation twins. The high-pressure experiments reveal that deformation twins: (i) promote the α-to-ω phase transformation by lowering the critical pressure for the phase transformation and (ii) stabilize the ω-phase, such that most of it is retained when the pressure reverses to ambient condition. Based on calculations of the local twin stresses and their influence on the strain energy associated with the α-to-ω phase transformation, we show that the local stress state produced within and around the deformation twins energetically favors the α-to-ω phase transformation and suppresses the reverse ω-to-α transformation upon pressure release.

2. Experimental details

To study the effect of deformation twins on the α-to-ω phase transformation, we prepare three different samples with and without deformation twins for the high-pressure experiments. The initial material for this study is high-purity crystal bar Zr (<100 ppm) arc-melted, cast into an ingot, and clock-rolled at room temperature with a strong basal texture and twin-free equiaxed grains with an average diameter of 17 microns (see Fig. 1(a)). The chemical composition of other elements O, C, N, Fe, Al, V, Hf and Ti (in ppm) is <50, 22, <20, <50, <20, <50, 35 and <25, respectively [29]. Cylindrical compression specimens were machined from the rolled plate and annealed at 550°C for 1hr. Twinned samples are made by compression deformation at 77K to a strain of either 5% or 10%. Electron Back Scatter Diffraction (EBSD) is used to identify and measure the twin volume fractions. Tensile twins of the $\{10-12\}\langle 1-101\rangle$ type is formed in the 5% and 10% strained samples, with associated volume fractions of 5% and 16%, respectively [30]. A relatively small number of $\{11\bar{2}1\}$tensile twins was reported, representing a volume fraction of less than 2% in the 10% strained sample [31]. Thus, only $\{10\bar{1}2\}$ tensile twins are considered in the present study. EBSD images in Figs. 1b

and 1c show that the twin thickness is much smaller than the grain size and most twinned grains contain multiple twin lamellae [30].

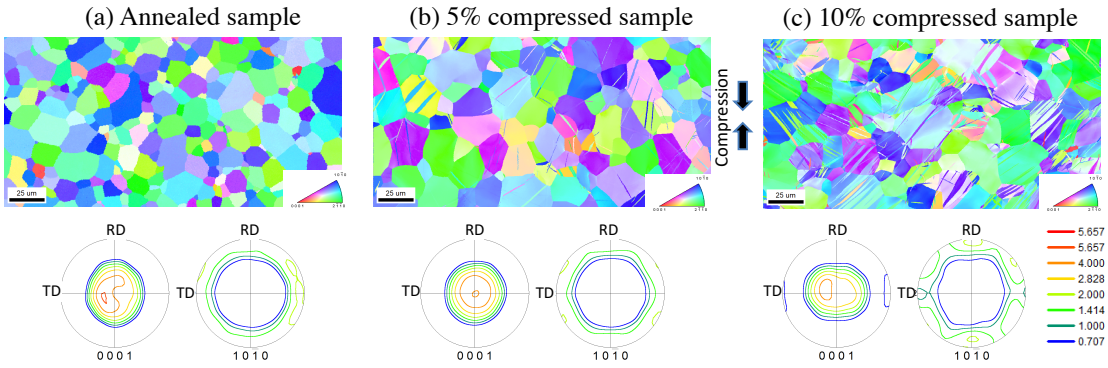

Figure 1. *Orientation maps (standard stereographic triangle showing rolling directions, RD) and pole figures of crystal orientations of the (a) annealed (twin-free microstructure), (b) 5% and (c) 10% pre-strained (twinned microstructures) Zr samples. Orientation map sections normal to RD. Annealed Zr possesses a strong basal texture. Pre-compression is applied along the transverse direction, TD (vertical in the orientation map) at 77K to activate* $\{10\bar{1}2\}$ *tensile twins. The twin volume fractions in the 5% and 10% compressed samples are measured using EBSD and determined to be 5% and 16%, respectively.*

Controlled hydrostatic pressure experiments are carried out on all three Zr samples: the annealed (twin-free) and the 5% and 10% pre-strained (twinned) samples. For these tests, a multi-anvil apparatus, the Deformation-DIA (D-DIA), at beam line 13-BM-D of the Advanced Photon Source at Argonne National Laboratory is used [31]. D-DIA consists of three pairs of mutually perpendicular carbide anvils with square tips of 3 mm that can be controlled independently to ensure a condition of hydrostatic pressure. This setup can also be used to impose deviatoric stresses at high pressures. Two vertical anvils are fixed to lower and upper guide blocks while the other two pairs of wedge shaped thrust anvils are in the horizontal plane and at 90° to each other (Figure 2(a)).

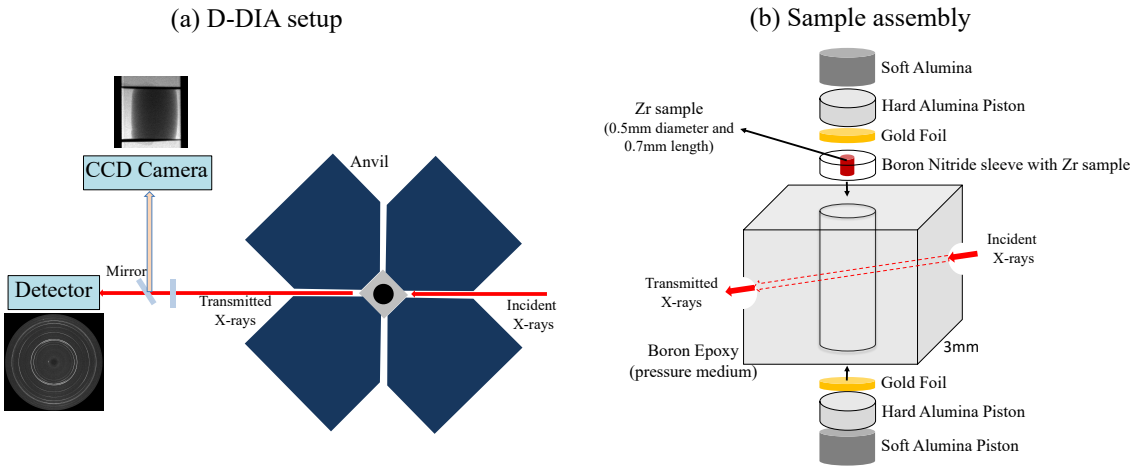

Figure 2. *D-DIA high pressure experiment setup and sample assembly. (a) Schematic representation of the D-DIA setup used for high pressure experiments at APS 13-BM-D. Here only four horizontal anvils are shown. The sample assembly is placed at the center of the D-DIA setup, and the X-ray beam passes through the entire sample assembly. Radiographic images and diffraction patterns are collected using a CCD camera and detector, respectively. (b) Schematic representation of the sequence in which a Zr-sample is placed along with other components inside the Boron Epoxy pressure medium.*

A small-sized assembly is compressed using differential hydraulic rams in a controlled manner to impose hydrostatic pressure while minimizing deviatoric stresses [31] (Figure 2(b)). The assembly is shaped as a cube located between the six anvils in a configuration that enables the anvils to make perfect contact with each face of the sample assembly. Due to the symmetry imposed by the guide blocks combined with the differential ram and anvils capabilities, the cubic sample assembly allows one to impose equal strain in all directions and thus a dilatational deformation. However, to guarantee a pure hydrostatic pressure state, fine-tuned corrections are applied manually on the lateral pistons in order to control the differential stress throughout the duration of the experiment. Because of the low rate of deformation required for evenly transmitting and equilibrating the pressure applied to the sample during loading and unloading, each experiment lasts about 11 hours.

The outer portion of the sample assembly is the pressure medium consisting of a 3 mm boron-epoxy cube containing a sample chamber stacked with the following

materials: crushable alumina, sintered alumina, a thin gold sheet, the Zr sample surrounded by a Boron Nitride sleeve, a thin gold sheet, sintered alumina, and crushable alumina. The thin gold sheets are used as markers to follow the axial straining of the sample. Pyrophyllite gaskets at the edges of the Boron Epoxy cube are used to maintain alignment of the sample with the x-ray beam.

The test samples consist of cylindrical specimens of 0.5 mm diameter and 0.8 mm length fabricated by an Electric Discharge Machining (EDM) process. The axial direction of the samples is the in-plane compression direction along which the samples were pre-strained. A 0.2066 Å wavelength X-ray beam collimated to 200 x 200 microns is used to obtain diffraction signals from the Zr sample. The diffraction images are recorded with a charge-coupled detector binned to 2048 x 2048 pixels (pixel size of 0.079 mm) for 200 seconds (see Figure 2(a)). Diffraction from the alumina pistons is simultaneously recorded for calibration and pressure estimation. Sample images are collected using an X-ray radiographic camera and the contrast provided by the gold sheets is used to calculate the strain imposed on the sample. Collected diffraction images are analyzed by the Rietveld method using the software MAUD, which fits the diffraction profiles while minimizing the difference between the experimental observation and model predicted crystal structures and microstructural characteristics [32-34]. The post-processing of diffraction images provides the evolution of phase fraction and texture.

3. Results and discussion

Hydrostatic pressure was imposed on the Zr samples in a controlled slow-rate fashion (typically at a strain rate of $10^{-5}s^{-1}$), and about five diffraction images were recorded for every 1 GPa pressure increment. The pressure corresponding to each diffraction image was calculated by fitting the unit cell parameters of both α and ω-Zr using the Birch-Murnaghan isothermal equations of state [35]. The diffraction images of the alumina piston were also used for pressure estimation. We find that the difference in pressure estimates obtained between the alumina and Zr diffraction images is within 0.2 GPa. The maximum uncertainties in pressure are estimated to be no larger than 0.3 GPa, with higher values associated with higher pressures.

Figure 3 shows selected X-ray diffraction patterns integrated over the full azimuthal range for all three samples at different pressures. Individual diffraction peaks of both α and ω phases are indicated with blue and red dashed lines, respectively, and important peaks are labeled with their Miller indices. At the beginning of the experiment (P=0.0001 GPa), all three samples' diffraction patterns exhibit only α-peaks. The diffraction patterns did not change significantly up to about 4 GPa for all three samples as shown in Figure 3. This indicates that the texture did not change with pressure, confirming indirectly that the samples experienced no relevant deviatoric stress components and the pressure did not induce deformation twinning. When the pressure increases to ~4.5 GPa, peaks in the diffraction pattern corresponding to ω-Zr appear in the pre-compressed (twinned) samples only. With increasing pressure, the intensities of the α-Zr peaks decrease and those of the ω-Zr peaks increase in all three samples. At around 7.5 GPa, the α-phase fully transforms into the ω-phase.

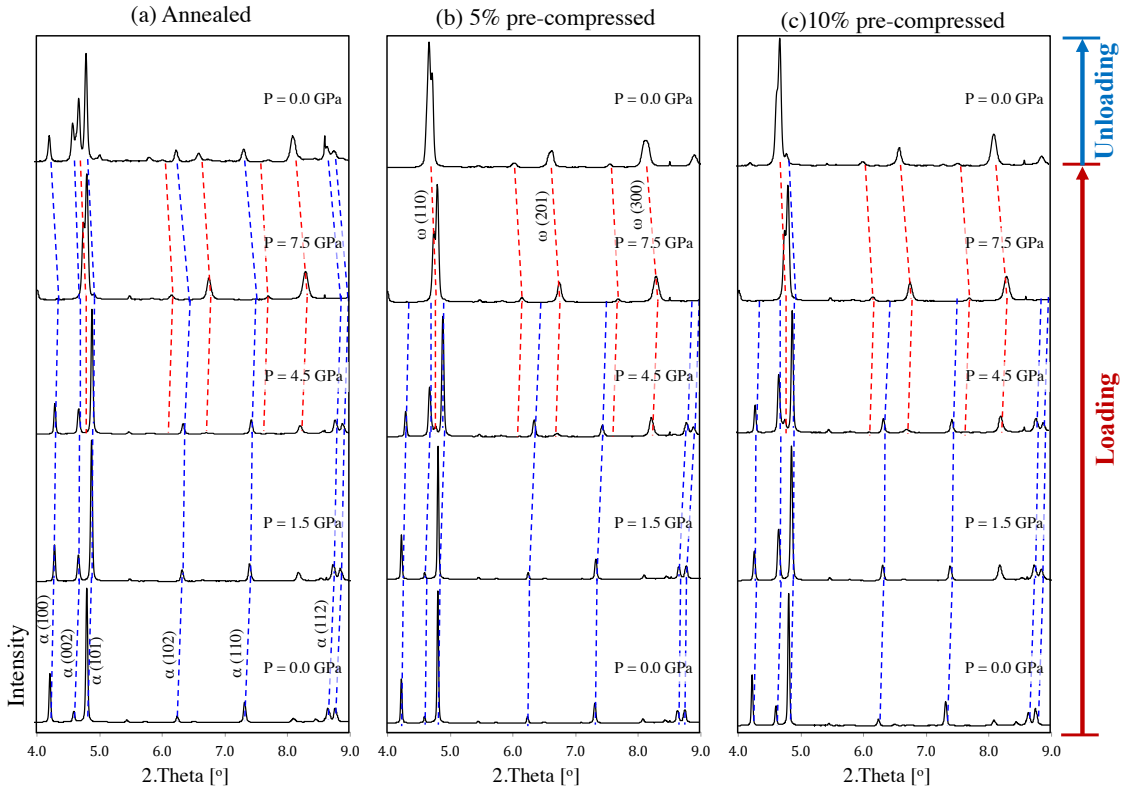

Figure 3. *Evolution of diffraction peaks with pressure. X-ray diffraction patterns of zirconium at different pressures: 0.0001, 1.5, 4.5, 7.5 GPa and 0.0001 GPa (after*

pressure release) for (a) annealed (twin-free), (b) 5% and (c) 10 % pre-compressed (twinned) samples. The blue and red lines follow the evolution and shift of diffraction peaks for α and ω phases, respectively. The signature of ω-phase starts to appear at around 4.5 GPa.

3.1. Effect of twinning microstructure

The corresponding volume fractions of the α-phase and the ω-phase were calculated using the Rietveld method [33, 34]. Figure 4 shows the evolution of the ω-phase volume fraction with pressure for all three samples. The maximum uncertainty in the volume fraction is estimated to be no larger than 8%. In this analysis, the pressure at which the ω-phase starts to appear is referred to as the *transformation start* pressure and the pressure at which all α-Zr transforms into ω-Zr is denoted as the *transformation end* pressure. The transformation start pressure of the annealed Zr sample is 5.2 GPa, significantly greater than that of the pre-compressed twinned samples, which are 4.0 GPa and 4.2 GPa for the 5% and 10% pre-compressed samples, respectively. The transformation end pressures for the annealed and 5% and 10% pre-compressed twinned samples are 8.0, 7.4 and 7.5 GPa, respectively. Note that once the transformation start pressure is reached, the phase transformation progresses rapidly and becomes complete within about 3 GPa. These measurements indicate that the presence of twins lowers the pressure for the α-to-ω phase transformation.

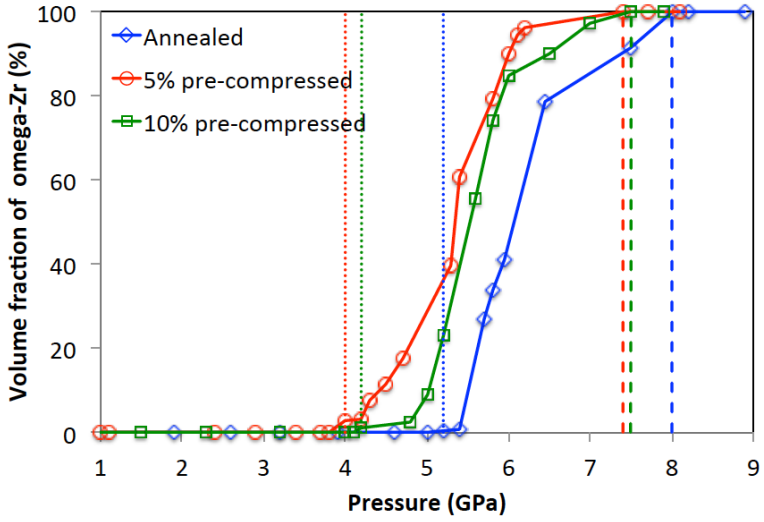

Figure 4. *Evolution of ω-phase volume fraction as a function of imposed pressure for all three samples. The vertical lines represent the transformation start and end pressures for the α-to-ω phase transformation. Both the transformation start and end pressures are lower for the twinned samples compared to twin-free sample.*

The diffraction profile of all three samples after releasing the pressure to ambient conditions are shown in the top row of Figure 3. They clearly show that the pre-twinned samples mostly contain ω-phase whereas the annealed un-twinned sample is comprised of both ω and α-phases. Quantitatively, Figure 5(a) shows the measured percentage of retained ω-phase in all three samples at ambient condition. The volume fraction of retained ω-phase in the twin free sample is 24% whereas in the twinned samples it is above 90%. To confirm, additional post-mortem EBSD imaging is performed on all three tested samples to analyze the retained ω-phase. For example, Figures 5(b)-(d) show the EBSD images of the retained α+ω, ω, and α-phases, respectively, for the 10% pre-compressed sample. The black regions in Figure 5(b) correspond to poorly indexed points. Consistent with the *in-situ* X-ray diffraction results, the area fraction of the retained ω-phase given by EBSD is high in the twinned samples compared to the twin-free sample. Quantitative values are affected by the large uncertainties associated with the non-indexed points and are not reported here.

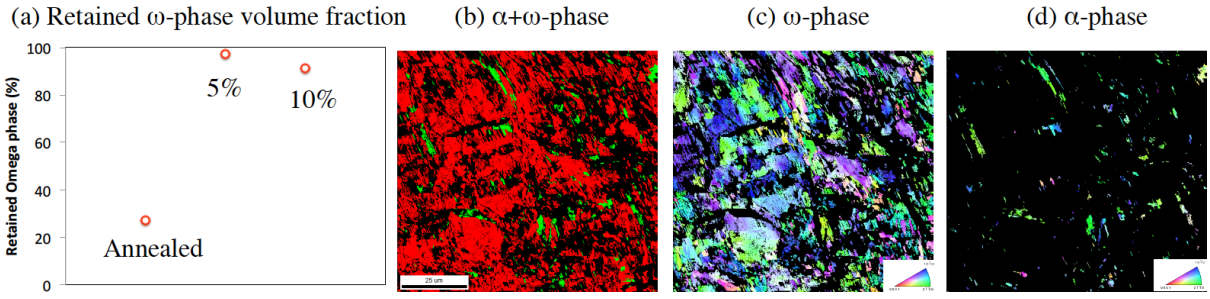

Figure 5. *Effect of twinning on the retention of ω-phase. (a) Volume fraction (%) of retained ω-phase in the tested samples at ambient condition. The X-ray diffraction measurements are performed in the sample after releasing the pressure and removing the D-DIA anvils. (b), (c) and (d) EBSD images of the retained α+ω, ω, and α-phase microstructure, respectively, in the 10% pre-compressed sample. In (b) green and red*

colors denote α and ω phases, respectively. The amount of retained ω-phase is significantly higher in the initially twinned microstructures than the twin-free microstructure.

3.2 Twin induced stresses and α-to-ω phase transformation

The experimental evidence indicates that pre-existing twins favor the α-to-ω phase transformation and hinder the reverse transformation. Deformation twins are sub-granular domains that impart shear on the surrounding crystal and bear a distinctly different crystallographic orientation [30, 36]. Twin shear transformations induce a local internal stress field in the crystal around the twin [37]. These internal stresses superimpose on any externally applied field such as the applied pressure. The implication is that the twin-generated field may partially accommodate the strain associated with the α-to-ω phase transformation, thereby reducing the pressure required to induce the transformation in a perfect crystal. To calculate the micromechanical stress-fields produced by $\{10\bar{1}2\}$ tensile twins in an α-Zr crystal, we use a 3D crystal plasticity Fast Fourier Transform (CP-FFT) model [38, 39]. This model calculates the tensorial stress fields induced by the shear transformation and accounts for anisotropic elasticity and plastic relaxation via crystallographic slip. Figure 6(a) maps the calculated resolved shear stress component projected on the twin plane (TRSS) solely due to the formation of a tensile twin in α-Zr grain [39]. This shear stress component is most intense along the coherent twin boundary where it is negative and unfavorable to twin growth, but in the region ahead of the twin tip it is positive and favorable to twin propagation.

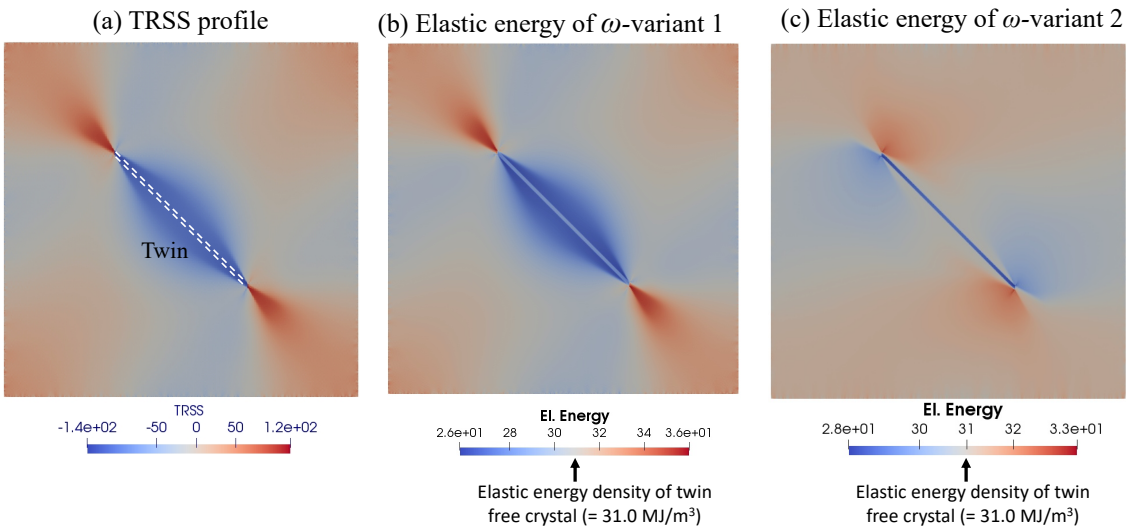

Figure 6. *Twin stresses and phase transformation. (a) Distribution of twin plane resolved shear stress (TRSS) in an HCP Zr grain after* $\{10\bar{1}2\}$ *tensile twin formation (in MPa) [39]. Elastic energy density (in MJ/m*^{3}*) associated with α-to-ω phase transformation taking place in the stress field of the twinned Zr at 5 GPa applied pressure for (b) ω- variant 1 and (c) ω-variant 2. Variant-3 is crystallographically equivalent to variant-2 and thus its energy profile is the same as the one of variant-2. The elastic energy density (MJ/m*^{3}*) associated with α-to-ω phase transformation of the twin-free crystal at 5 GPa pressure is given for comparison.*

To understand whether this twin-generated stress field favors or opposes the phase transformation, we calculate the energy associated with the α-to-ω transformation taking place in the presence of a twin induced stress field. We assume that the eigenstrain is accommodated elastically, in which case the elastic strain energy is given by $\mathrm{E} = \frac{1}{2}\sigma_{ij}\varepsilon_{ij}^{transf}$, where $\boldsymbol{\sigma}$ and $\boldsymbol{\varepsilon}^{transf}$ are the Cauchy stress tensor and α-to-ω transformation strain tensor, respectively. Although local plastic relaxation is likely to take place and partially relax the transformation-induced stress, the elastic component of the strain is still a good indicator of whether the twin-generated stress field favors the transformation. In the case of a perfect twin free crystal subject to hydrostatic pressure, the elastic energy density associated with the α-to-ω transformation is $E = \frac{1}{2}p\delta_{ij}\varepsilon_{ij}^{transf}$, the same anywhere in the domain of the crystal if the hydrostatic pressure, p ,is uniform.

The elastic energy for the phase transformation at different pressures can be determined by super-imposing the hydrostatic pressure components onto the stress state derived from the CP-FFT calculations. We choose the orientation relationship of the experimentally observed Silcock mechanism: $(0001)_\alpha||(11\bar{2}0)_\omega$; $[11\bar{2}0]_\alpha||[0001]_\omega$ [9, 40]. The transformation strain tensors for all three ω variants in a system where $X = [11\bar{2}0]_\alpha$; $Y = [0001]_\alpha$ and $Z = [1\bar{1}00]_\alpha$ are:

$$\boldsymbol{\varepsilon^1} = \begin{bmatrix} e_1 & 0 & 0 \\ 0 & e_2 & 0 \\ 0 & 0 & e_3 \end{bmatrix}; \quad \boldsymbol{\varepsilon}^2 = \boldsymbol{R\varepsilon}^1\boldsymbol{R}^T; \quad \boldsymbol{\varepsilon}^3 = \boldsymbol{R\varepsilon}^2\boldsymbol{R}^T \tag{1}$$

where $e_1 = \frac{(c_\omega - a_\alpha)}{a_\alpha}, e_2 = \frac{(a_\omega - c_\alpha)}{c_\alpha}, e_3 = \frac{(2\sqrt{3}a_\omega - 3\sqrt{3}a_\alpha)}{3\sqrt{3}a_\alpha}$. a_α , c_α, and a_ω , c_ω are the lattice constants of the α and ω phases, respectively, and R is a rotation matrix, given by

$$\boldsymbol{R} = \begin{bmatrix} 1/2 & 0 & -\sqrt{3}/2 \\ 0 & 1 & 0 \\ \sqrt{3}/2 & 0 & 1/2 \end{bmatrix} \tag{2}$$

Figures 6(b) and (c) show the transformation energy for ω-phase variants 1 and 2, respectively, forming inside the α-phase at 5 GPa pressure. The result for the third variant is identical to that of the second variant due to crystal symmetry. The lattice constants of the α and ω phases at 5GPa pressure are: $a_\alpha = 3.177, c_\alpha = 5.105$, a_ω= 4.954 and $c_\omega = 3.106$ [6]. The calculated transformation energy distribution supports that the α-to-ω phase transformation is energetically favorable (requires less energy) at and in the vicinity of the coherent twin boundary for the first variant, and inside the twin domain for the second variant. For reference, the transformation energy for the same variants in the twin-free perfect crystal is given in Figure 6. Direct comparison of the transformation energy for the twin-free and twinned crystals clearly supports the conclusion that the presence of the tensile twin lowers the pressure required to induce the α-to-ω phase transformation, and more specifically, this transformation is more likely to take place next to the coherent twin interface or inside the twin domain.

An interesting and potentially relevant result is the clear distinction between the formation of ω-phase variant 1 and variant 2. The former transformation is predicted to be favored outside the twin domain, while the latter would be favorable inside the twin domain. Either occurrence would lead to the formation of an α-ω interface. In addition,

it is plausible that both transformations take place simultaneously, in which case an ω-ω interface would form. We hypothesize that the stability of these interfaces would prevent the reverse ω-to-α transformation when the pressure is removed. An alternative, but not excluding, argument would be that the local stresses associated with the pre-existing tensile twin boundaries, although being altered after the forward α-to-ω phase transformation has taken place, retain the overall characteristic shown in Fig. 6. As a consequence, the reverse ω-to-α transformation would have to occur in an energy landscape where the sign is reversed with respect to a forward α-to-ω transformation, which should hinder the reverse transformation. The quantification of the local stresses associated with the transformation rely on the modeling of the plasticity of both α and ω crystals. Through extensive research over several decades, the plasticity of α-Zr is well known [18, 41-43]. On the other hand, the plasticity of the ω-phase is not yet well understood, and will be the subject of future studies.

3.3. Implications from this study and future directions

In this work we reveal a mechanism involving the coupling between deformation twins and the α-to-ω phase transformation in group IV transition metal zirconium. Based on the X-ray synchrotron experiment results and transformation energy calculation, we derive the following conclusions. When the twinned Zr is subjected to hydrostatic pressure, the stress fields in the vicinity of pre-existing twin boundaries help to trigger the phase transformation by lowering the pressure required for the phase transformation compared to the annealed un-twinned case. Two scenarios are then possible, either only the matrix grains undergo transformation while the twin region retains the original α-phase, or both the matrix grain and the twin region undergo the phase transformation. From these measurements, it is not possible to definitively determine which scenario occurs. However, in both cases the twin boundaries will be retained either as an α-ω interface in the former scenario or as an ω-grain boundary in the latter. These interfaces will be either coherent α-ω or low energy ω-ω interfaces. We propose that if the interfacial energy of these boundaries is lower compared to the original twin boundary, the ω-phase will be difficult to revert back to the α-phase upon the pressure reversal. However, confirmation requires atomistic calculations that will be considered in the

future. In contrast, when the annealed-Zr sample (twin-free) is subjected to hydrostatic pressure, it transforms the entire α-grain into possibly up to three ω-orientations separated by ω-ω interfaces. Upon pressure release, it is apparent from the experiment that the reverse transformation is accomplished more easily than when twins are present. This explanation supports our previous speculations in connection with shock loading or HPT tests. Under both shock loading and HPT, α-grains may twin first and afterwards pressure may trigger the phase transformation at and in the vicinity of twin boundaries. Those interfaces may help to stabilize the ω-phase at ambient conditions.

The knowledge acquired here has implications beyond the specific Zr system and conditions addressed in this work. For example, the high strength and high ductility of metastable Ti alloys with high content of V, Mo, and Nb is due to both stress-induced ω phase transformation and stress-induced twinning that take place under standard forming conditions [44, 45] . It may also point to a potential role of twinning on the formation of ω phase under shock-loading or high torsion pressure of Zr and Ti [7, 12]. As mentioned before, this work sheds light on phase transformations in other systems like polycrystalline Fe (from α-to-ε) [22], rolled Ti (from HCP to FCC) [23], uranium dioxide [24], and the Cu/Ag system [25].

In the context of design of experiments, this work suggests a way to design a material with different proportions of stable ω-phase for further detailed characterization. To date, the understanding of structural properties of ω-phase is limited by its instability at ambient condition. Prior studies on shock loading and HPT methods produce samples containing high dislocation content and severely augmented and complex, uncontrolled microstructures. On the other hand, as we have shown here, using hydrostatic pressure experiments with twinned microstructures produces materials with controlled microstructure and defect content.

Apart from all these new findings and their relevance, the main limitation of this work is the use of polycrystalline average X-ray synchrotron technique to study the highly heterogenous α-to-ω phase transformation phenomena. A controlled in-situ spatially-resolved microstructural characterization technique required to completely understand the local microstructure-governed phase transformation will be performed in the future. Also, in this work, only a particular tensile twin and its effect on a phase

transformation is studied. To develop a comprehensive understanding, different types of twins and possible combinations of grain boundaries need to considered.

4. Conclusions

In this work, we have investigated the effect of microstructure on the α to ω phase transformation and the stability of ω-phase using controlled in-situ high-pressure experiments with X-ray synchrotron diffraction and crystal plasticity calculations. To this effect we used twinned and twin-free microstructure samples of high purity Zirconium. The experiment reveals that the pre-existing twinned microstructures lower the α-to-ω phase transformation pressure and increases the amount of retained ω-phase. Using crystal plasticity calculations, this phenomenon is explained by the stress field produced by twins on the surrounding crystal, which favors the phase transformation and hinders the reverse path. In addition, the presence of deformation twins stabilizes the ω-phase upon release of pressure as evidenced by the fact that the percentage of retained ω-phase at ambient condition after releasing the pressure is much higher in the twinned microstructure compared to twin free microstructure material. This result is also confirmed by post-mortem EBSD analysis of the recovered material.

Acknowledgments

This work was fully funded by the U.S. Dept. of Energy, Office of Basic Energy Sciences Project FWP 06SCPE401. This research used resources of the Advanced Photon Source, a U.S. Department of Energy (DOE) Office of Science User Facility operated for the DOE Office of Science by Argonne National Laboratory under Contract No. DE-AC02-06CH11357. NH was partly supported by the PNP INSU program. I.J.B. acknowledges financial support from the National Science Foundation Designing Materials to Revolutionize and Engineer our Future (DMREF) program (NSF CMMI-1729887).

References

[1] J.C. Jamieson, Crystal Structures of Titanium, Zirconium, and Hafnium at High Pressures, Science 140(3562) (1963) 72-73.
[2] Y.K. Vohra, S.K. Sikka, R. Chidambaram, Electronic-Structure of Omega Phase of Titanium and Zirconium, J Phys F Met Phys 9(9) (1979) 1771-1782.

[3] L. Saldana, A. Mendez-Vilas, L. Jiang, M. Multigner, J.L. Gonzalez-Carrasco, M.T. Perez-Prado, M.L. Gonzalez-Martin, L. Munuera, N. Vilaboa, In vitro biocompatibility of an ultrafine grained zirconium, Biomaterials 28(30) (2007) 4343-4354.
[4] Y.F. Bychkov, Y.N. Likhanin, V.A. Maltsev, Physical Properties of Zirconium Omega-Phase, Fiz Met Metalloved+ 36(2) (1973) 413-414.
[5] S.K. Sikka, Y.K. Vohra, R. Chidambaram, Omega-Phase in Materials, Prog Mater Sci 27(3-4) (1982) 245-310.
[6] A. Kumar, M.A. Kumar, I.J. Beyerlein, First-principles study of crystallographic slip modes in omega-Zr, Sci Rep-Uk 7 (2017) 8932.
[7] E.K. Cerreta, J.P. Escobedo, P.A. Rigg, C.P. Trujillo, D.W. Brown, T.A. Sisneros, B. Clausen, M.F. Lopez, T. Lookman, C.A. Bronkhorst, F.L. Addessio, The influence of phase and substructural evolution during dynamic loading on subsequent mechanical properties of zirconium, Acta Mater 61(20) (2013) 7712-7719.
[8] D. Errandonea, Y. Meng, M. Somayazulu, D. Hausermann, Pressure-induced alpha ->omega transition in titanium metal: a systematic study of the effects of uniaxial stress, Physica B 355(1-4) (2005) 116-125.
[9] H.R. Wenk, P. Kaercher, W. Kanitpanyacharoen, E. Zepeda-Alarcon, Y. Wang, Orientation Relations During the alpha-omega Phase Transition of Zirconium: In Situ Texture Observations at High Pressure and Temperature, Phys Rev Lett 111 (2013) 195701.
[10] J.Z. Zhang, Y.S. Zhao, P.A. Rigg, R.S. Hixson, G.T. Gray, Impurity effects on the phase transformations and equations of state of zirconium metals, J Phys Chem Solids 68(12) (2007) 2297-2302.
[11] B.M. Morrow, P.A. Rigg, D.R. Jones, F.L. Addessio, C.P. Trujillo, R.A. Saavedra, D.T. Martinez, E.K. Cerreta, Shock and Microstructural Characterization of the α-ω Phase Transition in Titanium Crystals, Journal of Dynamic Behavior of Materials 3(4) (2017) 526-533.
[12] M.T. Perez-Prado, A.A. Gimazov, O.A. Ruano, M.E. Kassner, A.P. Zhilyaev, Bulk nanocrystalline omega-Zr by high-pressure torsion, Scripta Mater 58(3) (2008) 219-222.
[13] A.P. Zhilyaev, I. Sabirov, G. Gonzalez-Doncel, J. Molina-Aldareguia, B. Srinivasarao, M.T. Perez-Prado, Effect of Nb additions on the microstructure, thermal stability and mechanical behavior of high pressure Zr phases under ambient conditions, Mat Sci Eng a-Struct 528(9) (2011) 3496-3505.
[14] N. Velisavljevic, G.N. Chesnut, L.L. Stevens, D.M. Dattelbaum, Effects of interstitial impurities on the high pressure martensitic alpha to omega structural transformation and grain growth in zirconium, J Phys-Condens Mat 23(12) (2011) 125402.
[15] R.G. Hennig, D.R. Trinkle, J. Bouchet, S.G. Srinivasan, R.C. Albers, J.W. Wilkins, Impurities block the alpha to omega martensitic transformation in titanium, Nat Mater 4(2) (2005) 129-133.
[16] A. Jayaraman, W. Klement Jr, G. Kennedy, Solid-solid transitions in titanium and zirconium at high pressures, Phys Rev 131(2) (1963) 644.
[17] M.K. Jacobsen, N. Velisavljevic, S.V. Sinogeikin, Pressure-induced kinetics of the alpha to omega transition in zirconium, J Appl Phys 118(2) (2015) 025902.

[18] S.G. Song, G.T. Gray, Influence of Temperature and Strain-Rate on Slip and Twinning Behavior of Zr, Metall Mater Trans A 26(10) (1995) 2665-2675.
[19] P. Hazell, G. Appleby-Thomas, E. Wielewski, J. Escobedo, The shock and spall response of three industrially important hexagonal close-packed metals: magnesium, titanium and zirconium, Philosophical Transactions Of the Royal Society A: Mathematical, Physical and Engineering Sciences 372(2023) (2014) 20130204.
[20] T.S.E. Low, D.W. Brown, B.A. Welk, E.K. Cerreta, J.S. Okasinski, S.R. Niezgoda, Isothermal annealing of shocked zirconium: Stability of the two-phase alpha/omega microstructure, Acta Mater 91 (2015) 101-111.
[21] H.X. Zong, X.D. Ding, T. Lookman, J. Sun, Twin boundary activated alpha -> omega phase transformation in titanium under shock compression, Acta Mater 115 (2016) 1-9.
[22] N. Gunkelmann, E.M. Bringa, D.R. Tramontina, C.J. Ruestes, M.J. Suggit, A. Higginbotham, J.S. Wark, H.M. Urbassek, Shock waves in polycrystalline iron: Plasticity and phase transitions, Phys Rev B 89(14) (2014) 140102.
[23] H.C. Wu, A. Kumar, J. Wang, X.F. Bi, C.N. Tome, Z. Zhang, S.X. Mao, Rolling-induced Face Centered Cubic Titanium in Hexagonal Close Packed Titanium at Room Temperature, Sci Rep-Uk 6 (2016) 24370.
[24] T.G. Desai, P. Nerikar, B.P. Uberuaga, The role of grain boundary structure in stress-induced phase transformation in UO2, Model Simul Mater Sc 17(6) (2009) 064001.
[25] T. Frolov, M. Asta, Y. Mishin, Segregation-induced phase transformations in grain boundaries, Phys Rev B 92(2) (2015) 02103.
[26] X. Wang, L. Li, W. Mei, W. Wang, J. Sun, Dependence of stress-induced omega transition and mechanical twinning on phase stability in metastable β Ti–V alloys, Mater Charact 107 (2015) 149-155.
[27] L. Li, W. Mei, H. Xing, X. Wang, J. Sun, Zigzag configuration of mechanical twin and stress-induced omega phase in metastable β Ti–34Nb (at.%) alloy, J Alloy Compd 625 (2015) 188-192.
[28] Y. Yang, P. Castany, E. Bertrand, M. Cornen, J. Lin, T. Gloriant, Stress release-induced interfacial twin boundary ω phase formation in a β type Ti-based single crystal displaying stress-induced α" martensitic transformation, Acta Mater 149 (2018) 97-107.
[29] G.C. Kaschner, G.T. Gray, The influence of crystallographic texture and interstitial impurities on the mechanical behavior of zirconium, Metallurgical and Materials Transactions A 31(8) (2000) 1997-2003.
[30] L. Capolungo, P.E. Marshall, R.J. McCabe, I.J. Beyerlein, C.N. Tome, Nucleation and growth of twins in Zr: A statistical study, Acta Mater 57(20) (2009) 6047-6056.
[31] Y.B. Wang, W.B. Durham, I.C. Getting, D.J. Weidner, The deformation-DIA: A new apparatus for high temperature triaxial deformation to pressures up to 15 GPa, Rev Sci Instrum 74(6) (2003) 3002-3011.
[32] L. Lutterotti, S. Matthies, H.R. Wenk, A.S. Schultz, J.W. Richardson, Combined texture and structure analysis of deformed limestone from time-of-flight neutron diffraction spectra, J Appl Phys 81(2) (1997) 594-600.

[33] L. Lutterotti, R. Vasin, H.R. Wenk, Rietveld texture analysis from synchrotron diffraction images. I. Calibration and basic analysis, Powder Diffr 29(1) (2014) 76-84.
[34] H.R. Wenk, L. Lutterotti, P. Kaercher, W. Kanitpanyacharoen, L. Miyagi, R. Vasin, Rietveld texture analysis from synchrotron diffraction images. II. Complex multiphase materials and diamond anvil cell experiments, Powder Diffr 29(3) (2014) 220-232.
[35] Y.S. Zhao, J.Z. Zhang, C. Pantea, J. Qian, L.L. Daemen, P.A. Rigg, R.S. Hixson, G.T. Gray, Y.P. Yang, L.P. Wang, Y.B. Wang, T. Uchida, Thermal equations of state of the alpha, beta, and omega phases of zirconium, Phys Rev B 71(18) (2005) 184119.
[36] M.A. Kumar, M. Wroński, R.J. McCabe, L. Capolungo, K. Wierzbanowski, C.N. Tomé, Role of microstructure on twin nucleation and growth in HCP titanium: A statistical study, Acta Mater 148 (2018) 123-132.
[37] M.A. Kumar, B. Clausen, L. Capolungo, R.J. McCabe, W. Liu, J.Z. Tischler, C.N. Tome, Deformation twinning and grain partitioning in a hexagonal close-packed magnesium alloy, Nat Commun 9 (2018) 4761.
[38] M.A. Kumar, A.K. Kanjarla, S.R. Niezgoda, R.A. Lebensohn, C.N. Tome, Numerical study of the stress state of a deformation twin in magnesium, Acta Mater 84 (2015) 349-358.
[39] M.A. Kumar, I.J. Beyerlein, C.N. Tome, Effect of local stress fields on twin characteristics in HCP metals, Acta Mater 116 (2016) 143-154.
[40] H.X. Zong, T. Lookman, X.D. Ding, C. Nisoli, D. Brown, S.R. Niezgoda, S. Jun, The kinetics of the omega to alpha phase transformation in Zr, Ti: Analysis of data from shock-recovered samples and atomistic simulations, Acta Mater 77 (2014) 191-199.
[41] A. Akhtar, Teghtsoo.A, Plastic Deformation of Zirconium Single Crystals, Acta Metall Mater 19(7) (1971) 655-663.
[42] C. Tome, R. Lebensohn, U. Kocks, A Model for texture development dominated by deformation twinning - application to zirconium alloys, Acta Metallurgica Et Materialia 39(11) (1991) 2667-2680.
[43] I.J. Beyerlein, C.N. Tome, A dislocation-based constitutive law for pure Zr including temperature effects, Int J Plasticity 24(5) (2008) 867-895.
[44] M. Ahmed, D. Wexler, G. Casillas, O.M. Ivasishin, E.V. Pereloma, The influence of β phase stability on deformation mode and compressive mechanical properties of Ti–10V–3Fe–3Al alloy, Acta Mater 84 (2015) 124-135.
[45] M. Ahmed, D. Wexler, G. Casillas, D.G. Savvakin, E.V. Pereloma, Strain rate dependence of deformation-induced transformation and twinning in a metastable titanium alloy, Acta Mater 104 (2016) 190-200.